The Ionic Hydrogen Bond. 5. Polydentate and Solvent-Bridged Structures. Complexing of the Proton and the Hydronium Ion by Polyethers

Michael Meot-Ner (Mautner),† L. Wayne Sieck,*,† Steve Scheiner,‡ and Xiaofeng Duan‡

Contribution from the Chemical Kinetics and Thermodynamics Division, National Institute of Standards and Technology, Gaithersburg, Maryland 20899, and Department of Chemistry and Biochemistry, Southern Illinois University at Carbondale, Carbondale, Illinois 62901-4409

Received April 26, 1993. Revised Manuscript Received May 16, 1994®

Abstract: The thermochemistry associated with protonated complexes containing one or two glyme ($MeOCH_2CH_2OMe$, (G1)), diglyme ($Me(OCH_2CH_2)_2OMe$, (G2)), or triglyme ($Me(OCH_2CH_2)_3OMe$ (G3)) molecules and 0–3 H_2O molecules was measured by pulsed high-pressure mass spectrometry. Comparison of polyether, crown ether, and acetone complexes with H^+ and H_3O^+ shows increasing binding energies with increasing flexibility in the ligands. For example, in protonated clusters containing ligands with a total of four polar groups, the proton is bonded by a total energy of (kJ/mol (kcal/mol)): four Me_2CO molecules, 1044.8 (249.7); two G1 molecules, 987.4 (236.0); one G3 molecule, 962.3 (230.0); 12-crown-4, 941.4 (225.0). Stabilization of the proton by dipoles of the free ether groups contributes significantly; for example, 17 and 54 kJ/mol (4 and 13 kcal/mol) in the binding energy within $(G1)_2H^+$ and $(G2)_2H^+$ dimers, respectively. The thermochemistry of H_3O^+ binding indicates bidentate complexes with one each of G2, G3, and 15-crown-5 molecules and two G1 molecules, with binding energies of 310–352 kJ/mol (74–84 kcal/mol). In these complexes the second $OH^+\cdot O$ bond contributes up to 113 kJ/mol (27 kcal/mol). Larger binding energies of 387–475 kJ/mol (93–99 kcal/mol) indicate tridentate complexes of H_3O^+ with two G1 and two G3 molecules, as well as with 18-crown-6, which is the best complexing agent due to entropy effects. In complexes containing additional water molecules, the thermochemistry suggests that two H_2O molecules form a protonated solvent bridge between ether groups in $(G1\cdot 2H_2O)H^+$ and $(G3\cdot 2H_2O)H^+$. Ab initio calculations show that open and solvent-bridged structures have comparable energies (within 16 kJ/mol (4 kcal/mol)). The calculated barriers to direct and solvent-mediated proton transfer between functional groups are 0–16 kJ/mol (0–4 kcal/mol). The solvent-bridged structures are models for water chains involved in proton transport in biomembranes.

Introduction

The protonation and clustering of polydentate molecules generates complex ionic hydrogen-bonded systems.[1-7] For example, internal hydrogen bonds (IHB) are formed upon the protonation of polyamines,[1,4] polyethers,[2,5] diketones,[5] and amino acid derivatives.[7] The strengths of the internal bonds can be estimated by comparison with monofunctional molecules.[4,5] The results show internal hydrogen bonds as strong as 100 kJ/mol (24 kcal/mol). The cyclic structures also lead to large negative entropies of protonation, up to -80 J/(mol K) (-19 cal/(mol K).

The bonding of polyfunctional molecules with polyprotonic ions forms multiply hydrogen-bonded structures.[3,6,8] Thermochemical evidence for multiple interactions was found, for example, in complexes of protonated amines with polyethers[7] and in the complexing of H_3O^+ by crown ethers.[3] An earlier review has summarized some these effects.[8] In this work, we will evaluate the energy factors involved in the polydentate complexing of H_3O^+, as well as further hydration and solvation.

Despite the interesting structural effects in internally or multiply hydrogen-bonded gas-phase complexes, few studies have been reported. No systems have been studied simultaneously incorporating several polyfunctional molecules. The present work will also address such clusters.

Hydrogen-bonded cluster ions can serve as models for bioenergetics. For example, we developed models of ionic interactions at active enzyme centers[9] and of water wires[10] that were postulated to transport protons in biomembranes.[11] The present results are also pertinent in this respect, since polyethers are similar to the polar environments of protein interiors[12] and solvent-bridged structures may be involved in proton transport.

This article will compare the complexing energies of H^+ and H_3O^+ with several polar oxygen groups, either when located on separate free molecules or when constrained in one or more polyfunctional ligands. We shall also evaluate the contributions of various energetic factors and use ab initio calculations to assess the relative energies and optimum geometries of model systems.

Experimental and Theoretical Methods

Thermochemical measurements were performed using the NIST pulsed high-pressure mass spectrometer. The instrument and the technique were described in detail recently.[13] Gas mixtures of 10^{-3} to 3×10^{-2} mole fraction (m.f.) H_2O or CH_3OH and 10^{-5} to 10^{-3} m.f. ether in N_2 carrier gas and trace $CHCl_3$ for electron capture were prepared in a 3 L glass bulb heated to 150 °C and allowed to flow to the ion source through glass and stainless steel lines also heated to 150 °C. The total pressure in the ion source was 2–4 mbar. Gas mixtures were ionized by 1–2-ms pulses of 500–1000-eV electrons, and the equilibrium ion intensities were monitored for reaction times of 2–15 ms. See Appendix for additional experimental details.

† National Institute of Standards and Technology.
‡ Southern Illinois University at Carbondale.
* Abstract published in *Advance ACS Abstracts*, July 15, 1994.

(1) Yamdagni, R.; Kebarle, P. *J. Am. Chem. Soc.* **1973**, *95*, 3504.
(2) Sharma, R. B.; Blades, A. T.; Kebarle, P. *J. Am. Chem. Soc.* **1984**, *106*, 510.
(3) Sharma, R. B.; Kebarle, P. *J. Am. Chem. Soc.* **1984**, *106*, 3913.
(4) Meot-Ner (Mautner), M.; Hamlet, P.; Hunter, e. P.; Field, F. H. *J. Am. Chem. Soc.* **1980**, *102*, 6866.
(5) Meot-Ner (Mautner), M. *J. Am. Chem. Soc.* **1983**, *105*, 4906.
(6) Meot-Ner (Mautner), M. *J. Am. Chem. Soc.* **1983**, *105*, 4912.
(7) Meot-Ner (Mautner), M. *J. Am. Chem. Soc.* **1984**, *106*, 278.
(8) Meot-Ner (Mautner), M. *Acc. Chem. Res.* **1984**, *17*, 186.
(9) Meot-Ner (Mautner), M. *J. Am. Chem. Soc.* **1988**, *110*, 3071.
(10) Meot-Ner (Mautner), M. *J. Bioenerg. Biomembr.* Submitted for publication.
(11) Nagle, J. F.; Tristram-Nagle, S. *J. Membr. Biol.* **1983**, *74*, 1.
(12) Warshel, A. *Acc. Res.* **1981**, *14*, 284.
(13) Meot-Ner (Mautner), M.; Sieck, L. W. *J. Am. Chem. Soc.* **1991**, *113*, 4448.

0002-7863/94/1516-7848$04.50/0

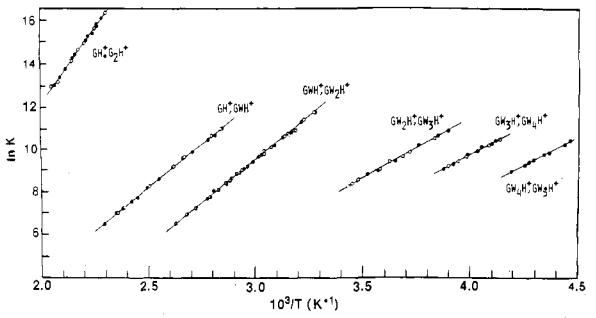

Figure 1. van't Hoff plots for association reactions in glyme (G)/water (W) mixtures. GW_2H^+, GW_3H^+ denotes $GW_2H^+ + W \leftrightarrow GW_3H^+$, etc. The variously marked points indicate mixtures of different concentrations. Standard state = 1 bar.

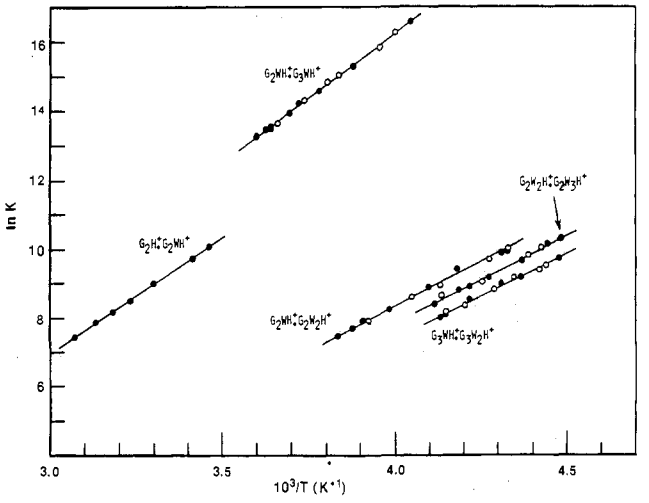

Figure 2. van't Hoff plots for association reactions in glyme (G)/water (W) mixtures. GW_2H^+, GW_3H^+ denotes $GW_2H^+ + W \leftrightarrow GW_3H^+$, etc. The variously marked points indicate mixtures of different concentrations. Standard state = 1 bar.

Ab initio calculations were performed using *Gaussian-88* and *-90* suites of computer programs.[14] The 4-31G basis set[15] was chosen both because of its computational efficiency and for its proven ability to deal with hydrogen bonds and proton-transfer energetics in a satisfactory manner.[16-18]

Results

Van't Hoff plots for the various association reactions are presented in Figures 1–5, and the thermochemical results are presented in Table 1. In eight sets of replicate measurements, the average standard deviation was ±1.7 kJ/mol (±0.4 kcal/mol) in $\Delta H°$ and ±5.0 J/(mol K) (±1.2 cal/(mol K)) in $\Delta S°$. We assign to the errors the usual values in such measurements, which are ±4 kJ/mol (±1 kcal/mol) for $\Delta H°$ and ±8 J/(mol K) (±2 cal/(mol K)) for $\Delta S°$.

The most likely source of systematic error would be the pyrolysis of the protonated or neutral ethers.[19] The present experiments were conducted at moderate temperatures, mostly below 400 K,

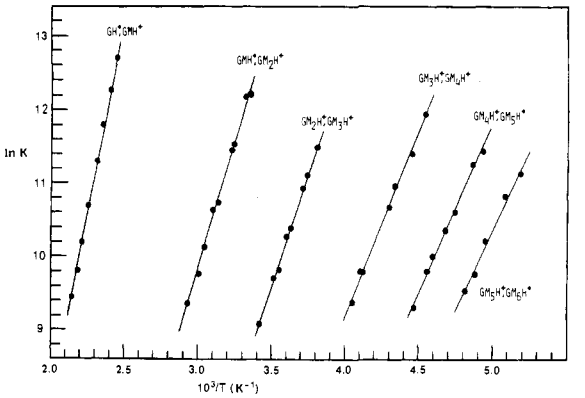

Figure 3. van't Hoff plots for association reactions in glyme (G)/MeOH (M) mixtures. GW_2H^+, GW_3H^+ denotes $GW_2H^+ + W \leftrightarrow GW_3H^+$, etc. Standard state = 1 bar.

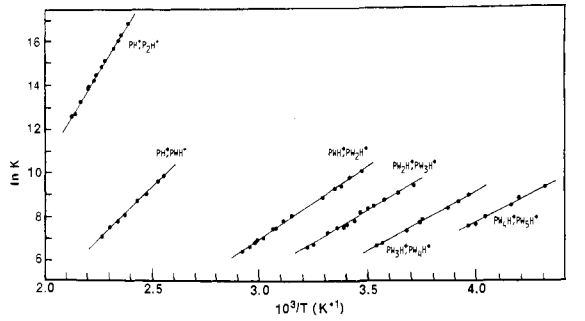

Figure 4. van't Hoff plots for association reactions in propyl ether (P)/water (W) mixtures. Standard state = 1 bar.

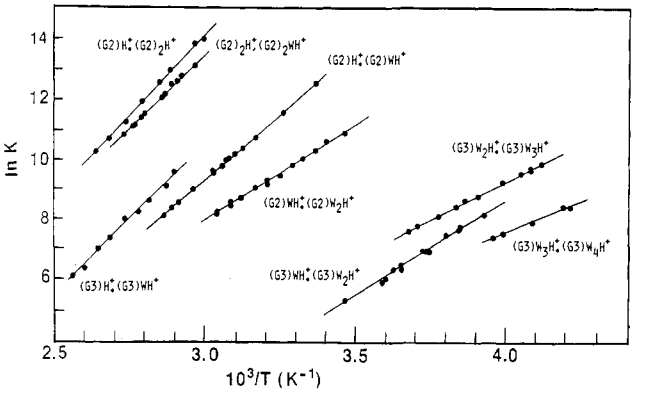

Figure 5. van't Hoff plots for association reactions in diglyme (G2)- or triglyme (G3)/water (W) mixtures. Standard state = 1 bar.

where this problem is minimized. In this context we note that our values for the $(G1)_2H^+$ dimer are substantially different than those of Sharma et al.[2] (see Table 1). The rates of pyrolysis of protonated diethers are known to increase rapidly above 500 K.[19] The van't Hoff plot for $(G1)_2H^+$ reported by Sharma et al. is based on four points only, two of which were taken at ~525 and ~575 K, and the plot appears to exhibit curvature. At those temperatures the unimolecular decomposition rates are approximately 2×10^2 and 1×10^3 s^{-1}, which are significant on the time scale of the experiment. The system is further complicated by the fact that the decomposition product $CH_3CHOCH_3^+$ slowly reprotonates G1 in a moderately endergonic reaction, $\Delta H°$ = +5.9 kJ/mol (+1.4 kcal/mol), $\Delta S°$ = −18 J/(mol K) (−4.3 cal/(mol K)). To avoid these complications, our measurements with this molecule were carried out at reduced temperatures of 425–485 K, and the van't Hoff plot appears to be linear in this range.

Sharma et al. used Me_2O as a monofunctional model for comparison with ether groups in polyethers.[2,3] However, the data available for Me_2O/H_2O mixed clusters shows some inconsistency

(14) Frisch, M. J.; Head-Gordon, M.; Schlegel, H. B.; Raghavachari, K.; Brinkley, J. S.; Gonzalez, C.; Jefrees, D. J.; Fox, D. J.; Whiteside, R. A.; Seeger, R.; Melius, C. F.; Baker, J.; Martin, R.; Kahn, L. R.; Stewart, J. J. P.; Fluder, E. M.; Topiol, S.; Pople, J. A. *Gaussian 88*; Gaussian, Inc.; Pittsburgh, PA, 1988. Frisch, M. J.; Head-Gordon, M.; Trucks, G. W.; Foresman, J. B.; Schlegel, H. B.; Raghavachari, K.; Robb, M. A.; Binkley, J. S.; Gonzalez, C.; Defrees, D. J.; Fox, D. J.; Whiteside, R. A.; Seeger, R.; Melius, C. F.; Baker, J.; Martin, R.; Kahn, L. R.; Stewart, J. J. P.; Topiol, S.; Pople, J. A. *Gaussian 90*; Gaussian, Inc.: Pittsburg, PA, 1990.

(15) Hehre, W. J.; Ditchfield, R.; Pople, J. A. *J. Chem. Phys.* **1972**, *56*, 2267.

(16) Meot-Ner (Mautner), M.; Cybulski, S. M.; Scheiner, S.; Liebman, J. F. *J. Phys. Chem.* **1988**, *92*, 2738.

(17) Cybulski, S. M.; Scheiner, S. *J. Phys. Chem.* **1990**, *94*, 6106.

(18) Scheiner, S. *Acc. Chem. Res.* **1985**, *18*, 174.

(19) Sieck, L. W.; Meot-Ner (Mautner), M. J. *Phys. Chem.* **1984**, *88*, 5324 and 5328.

Table 1. Thermochemistry of Association Reactions

	$-\Delta H°$		$-\Delta S°$	
	kJ/mol	kcal/mol	J/(mol K)	cal/(mol K)
	$BH^+ + B$			
$Me_2COH^+ + Me_2CO$	125.9[a]	30.1[a]	122.6[a]	29.3[a]
$Et_2COH^+ + Et_2CO$	130.5	31.2	149.5	35.7
$n\text{-}Pr_2OH^+ + n\text{-}Pr_2O$	129.4[b]	30.9[b]	167.4[b]	40.0[b]
$G1H^+ + G1$	114.6	27.4	129.3	30.9
	95.4[c]	22.8[c]	102.5[c]	24.5[c]
$G2H^+ + G2$	89.1	21.3	159.0	38.0
	$BH^+ + H_2O$			
$Me_2COH^+ + H_2O$	85.8[d]	20.5[d]	108.8[d]	26.0[d]
$n\text{-}Pr_2OH^+ + H_2O$	78.7	18.8	118.8	28.4
$G1H^+ + H_2O$	68.6	16.4	102.5	24.5
$G2H^+ + H_2O$	73.6	17.6	146.4	35.0
$G3H^+ + H_2O$	85.4	20.4	167.8	40.1
$(G2)_2H^+ + H_2O$	86.2	20.6	145.2	34.7
	$BH^+\cdot H_2O + H_2O$			
$Me_2COH^+\cdot H_2O + H_2O$	56.9[d]	13.6[d]	97.1[d]	23.2[d]
$n\text{-}Pr_2OH^+\cdot H_2O + H_2O$	55.2	13.2	107.5	25.7
$G1H^+\cdot H_2O + H_2O$	65.7	15.7	119.7	28.6
$G2H^+\cdot H_2O + H_2O$	54.8	13.1	97.1	23.2
$G3H^+\cdot H_2O + H_2O$	51.5	12.3	132.6	31.7
	$BH^+\cdot 2H_2O + H_2O$			
$Me_2COH^+\cdot 2H_2O + H_2O$	53.1	12.7	91.6	21.9
$n\text{-}Pr_2OH^+\cdot 2H_2O + H_2O$	52.3	12.5	113.0	27.0
$G1H^+\cdot 2H_2O + H_2O$	47.3	11.3	94.1	22.5
$G2H^+\cdot 2H_2O + H_2O$	42.7[e]	<10.2[e]	(105)[e]	(25)[e]
$G3H^+\cdot 2H_2O + H_2O$	43.1	10.3	95.8	22.9
	Higher Hydration			
$n\text{-}Pr_2OH^+\cdot 3H_2O + H_2O$	43.9	10.5	99.2	23.7
$n\text{-}Pr_2OH^+\cdot 4H_2O + H_2O$	42.6	10.2	105.9	25.3
$n\text{-}Pr_2OH^+\cdot 5H_2O + H_2O$	39.3[f]	9.4[f]	(105)[f]	(25)[f]
$G3H^+\cdot 3H_2O + H_2O$	38.1	9.1	88.7	21.2
	$G1H^+ + MeOH$			
$G1H^+ + MeOH$	92.0	22.0	118	28.3
$G1H^+\cdot MeOH + MeOH$	60.2	14.4	99	23.6
$G1H^+\cdot 2MeOH + MeOH$	52.7	12.6	105	25.0
$G1H^+\cdot 3MeOH + MeOH$	42.7	10.2	93	22.3
$G1H^+\cdot 4MeOH + MeOH$	38.5	9.2	93	22.2
$G1H^+\cdot 5MeOH + MeOH$	37.2	8.9	100	24.0

[a] Reference 30. [b] From the switching reaction $(Et_2CO)_2H^+ + 2(n\text{-}Pr_2O) \leftrightarrow (n\text{-}Pr_2O)_2H^+ + 2Et_2CO$, for which we measured $\Delta H° = -2.9$ kJ/mol and $\Delta S° = -14.5$ J/(mol K), and a thermochemical cycle using the proton-transfer reaction $Et_2COH^+ + n\text{-}Pr_2O \leftrightarrow n\text{-}Pr_2OH^+ + Et_2CO$, for which we measured $\Delta H° = -4.2$ kJ/mol and $\Delta S° = 3.1$ J/(mol K). [c] Reference 2. [d] Reference 29. [e] From $\Delta G_{257} > -15.9$ kJ/mol (−3.8 kcal/mol), $\Delta S°$ estimated. [f] From $\Delta G_{234} = -14.6$ kJ/mol (−3.5 kcal/mol), $\Delta S°$ estimated.

in thermochemical cycles.[20] The critical parameters in ionic hydrogen bonds are the proton affinities of the components, and in this respect the ether groups in the large polyethers are probably more similar to those in large ethers, such as $n\text{-}Pr_2O$, rather than to Me_2O. Another appropriate model may be Me_2CO, which has a proton affinity close to those of ethers such as MeOEt and Et_2O.[21] We have recent data on Me_2CO/H_2O protonated clusters from this laboratory, and we measured the thermochemistry associated with the $n\text{-}Pr_2O\cdot nH_2O$ hydration series in this study. These data will be used to model monodentate systems for comparison with the energetics of polydentate complexes.

Complexing of the Proton by One Polyfunctional Molecule. Table 2 lists the thermochemistries for complexing the proton by polyfunctional ligands with 2–6 functional groups.

In these systems, as in ions I and II, the hydrogen bond to a second functional group may be optimized or strained. Further stabilization may also be provided by the dipoles of additional ether groups, as discussed by Sharma et al.[2,3]

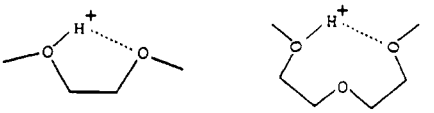

I II

The lowest complexing energy found for H^+ in Table 2 is in $G1H^+$ (ion I), which has only two oxygenated groups. The ab initio calculations for this system show a strained geometry which allows only a weak internal hydrogen bond. The strength of this bond has been previously estimated, by comparison with monofunctional bases, as 29 kJ/mol (7 kcal/mol).[5] The theoretical treatment indicates that the strength of the internal bond, compared with an open conformation, is 59.8 kJ/mol (14.3 kcal/mol). Compared with the case of optimized $OH^+\cdots O$ bonds, which exhibit strengths of 130 ± 8 kJ/mol (31 ± 2 kcal/mol), the strain effect is approximately 100 kJ/mol (24 kcal/mol).[2,5] Stronger internal bonds and reduced strain effects of 25 and 17 kJ/mol (6 and 4 kcal/mol) are associated with $G2H^+$ (ion II) and (12-crown-4)H^+, respectively. The ions (15-crown-5)H^+, (18-crown-6)H^+, and $G3H^+$ show similar or somewhat increased stabilization of H^+ compared with $(Me_2CO)_2H^+$ due to interactions of the additional polar groups.

Complexing of the Proton by Several Ligand Molecules. A. Enthalpy and Free Energy Effects. In complexes involving several ligand molecules, the data in Table 2 show that the stabilization of the proton increases with increasing freedom in the ligands in terms of $\Delta H°$ but concurrent entropy effects reduce the differences in terms of $\Delta G°$. When four oxygen functions are available, the $\Delta H°$ for proton complexing is lowest in (12-crown-4)H^+. The bond strength increases by 21.2 kJ/mol (5.0 kcal/mol) in the more flexible $G3H^+$ molecule, 46.0 kJ/mol (11.0 kcal/mol) in $(G1)_2H^+$, which has two free molecules that allow an optimized OH^+ bond (ion III), and 103.4 kJ/mol (24.7 kcal/mol) in $(Me_2CO)_4H^+$, which incorporates four free ligands. (A possible structure for the latter involves bonding of the last two Me_2CO molecules to methyl groups via $CH^+\cdots O$-type bonds.[22,23]) While the $\Delta H°$ values span a range of 100 kJ/mol (24 kcal/mol), the $\Delta G°_{300}$ values differ by only 34 kJ/mol (8 kcal/mol), reflecting the negative entropy effects as more free molecules are assembled to form the complex.

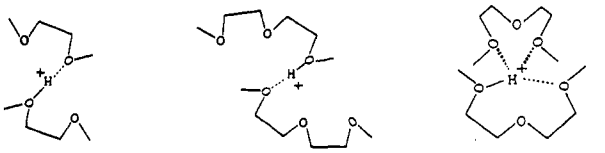

III IV IV'

Similarly, the effects of increasing geometry optimization are noted in systems with six polar groups. The proton is bonded most weakly by (18-crown-6)H^+, and the bonding increases by 46.5 kJ/mol (11.1 kcal/mol) in $(G2)_2H^+$ (two free molecules), by 51.9 kJ/mol (12.4 kcal/mol) in $(G1)_3H^+$ (three free molecules), and by 131 kJ/mol (31 kcal/mol) (estimated, see Table 2) in $(Me_2CO)_6H^+$ (six free ligand molecules). Again, the entropy effects associated with assembling the clusters decreases the differences in $\Delta G°_{300}$ to 9.2 kJ/mol (2.2 kcal/mol), 3.6 kJ/mol (0.9 kcal/mol), and 7 kJ/mol (2 kcal/mol), respectively. Overall, an 18-crown-6, two G1, three G1, two G2, four Me_2CO, and six Me_2CO molecules all appear to complex the proton comparably, with $\Delta G°_{300}$ values falling within a range of 17 kJ/mol (4 kcal/mol).

B. Energy Factors in Protonated Dimers. We note that the association energies (kJ/mol (kcal/mol)) to form $(G1)_2H^+$, −116.7 (−27.9), and $(G2)_2H^+$, −92.0 (−22.0) (ions III and IV), are smaller

(20) Hiraoka, K.; Grimsrud, E. P.; Kebarle, P. *J. Am. Chem. Soc.* **1974**, *96*, 3359.
(21) Lias, S. G.; Liebman, J. F.; Levin, R. D. *J. Phys. Chem. Ref. Data* **1984**, *13*, 695.
(22) Meot-Ner (Mautner), M.; Deakyne, C. A. *J. Am. Chem. Soc.* **1985**, *107*, 469.
(23) French, M. A.; Ikuta, S.; Kebarle, P. *Can. J. Chem.* **1982**, *60*, 1907.

Table 2. Thermochemistry of Complexation[a] of H^+ and H_3O^+

	$-\Delta H°$ [a]		$-\Delta S°$ [b]		$-\Delta G°_{300}$		
	kJ/mol	kcal/mol	J/(mol K)	cal/(mol K)	kJ/mol	kcal/mol	ref
			Complexation of H^+				
G1	873.2	208.7	126.7	30.3	835.1	199.6	2
	871.9	208.4	135.6	32.4	831.4	198.7	5
G2	932.6	222.9	166.5	39.8	882.8	211.0	2
	928.8	222.0	168.6	40.3	878.6	210.0	5
12-crown-4	941.4	225.0	143.6	34.3	888.3	212.3	5
15-crown-5	949.8	227.0	155.2	37.1	903.3	215.9	5
$2Me_2CO$	956.0	228.5	231.4	55.3	886.6	211.9	10
G3	962.3	230.0	186.6	44.6	906.7	216.7	2
	951.9	227.5	185.4	44.3	896.6	214.3	5
18-crown-6	978.2	233.8	200.8	48.0	918.4	219.5	2
2G1	987.4	236.0	254.0	60.7	911.2	217.8	28
	967.4	231.2	238.1	56.9	896.2	214.2	4
$3Me_2CO$	1004.2	240.0	323.8	77.4	907.1	216.8	10
$4Me_2CO$	1044.8	249.7	415.9	99.4	920.1	219.9	10
2G2	1024.7	244.9	324.3	77.5	927.6	221.7	
3G1	1030.1	246.2	359.0	85.8	922.0	220.4	28
$6Me_2CO$	(1113)[c]	(266)[c]	(628)[c]	(150)[c]	(925)[c]	(221)[c]	
			Complexation of H_3O^+				
bidentate complexes							
G1	245.2	58.6	125.5	30.0	207.5	49.6	28
$2Me_2CO$	308.4	73.7	239.7	57.3	236.4	56.5	10
G2	309.6	74.0	208.4	49.8	247.3	59.1	
G3	351.0	83.9	249.8	59.7	276.1	66.0	
15-crown-5	338.5	80.9	180.8	43.2	284.5	68.0	3
2G1	348.1	83.2	264.0	63.1	269.0	64.3	28
tridentate complexes							
$3Me_2CO$	385.8	92.2	364.0	87.0	276.6	66.1	10
18-crown-6	387.0	92.5	233.5	55.8	317.6	75.9	3
3G1	409.6	97.9	373.6	89.3	297.5	71.1	28
2G2	414.2	99.0	364.8	87.2	304.6	72.8	
$4Me_2CO$	(418)[c]	(100)[c]	(469)[c]	(112)[c]	(278)[c]	(66)[c]	
$6Me_2CO$	(484.9)[c]	(116)[c]	(673.0)[c]	(162)[c]	(282)[c]	(67)[c]	

[a] From cycle 3–5, using protonation thermochemistry from ref 16 for compounds below Me_2CO. For Me_2CO we use PA = 198.5 kcal/mol, and for the other compounds the values from the cited references are adjusted by +4 kcal/mol according to ref 13. Values are based on present results unless noted otherwise. [b] $\Delta S°$ values for protonation are assigned as –26 cal/(mol K) for a reference compound without symmetry changes, as in ref 16, plus $\Delta S°$ for proton transfer from such reference compounds to polyethers and crown ethers in the references quoted. For $Me_2COH^+ \cdot nMe_2CO$, the quoted value is –26 cal/(mol K) for $H^+ + Me_2CO$, plus the cumulative clustering entropies. [c] For addition of Me_2CO molecules to large clusters, we assume $\Delta H° = -8$ kcal/mol and $\Delta S° = -25$ cal/(mol K), on the basis that clustering thermochemistry usually approaches the bulk condensation thermochemistry.

than the usual -130 ± 8 (-31 ± 2) measured for $OH^+ \cdots O$ dimers due to the fact that the internal hydrogen bonds are broken during the dimerization process. The energy factors involved may be analyzed by the following scheme and eq 1.

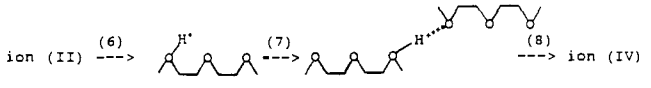

$$\Delta H°(\text{exp}) = -\Delta H°_{\text{IHB}} + \Delta H°_7 + \Delta H°_8 \qquad (1)$$

To form dimers III and IV, the intramolecular hydrogen bond (IHB) can be hypothetically assumed to first dissociate as in reaction 6. As in previous work, we assign $\Delta H°_6 = -\Delta H°_{\text{IHB}} =$ 29 (7) and 92 (22) kJ/mol (kcal/mol) in $G1H^+$ and $G2H^+$, respectively,[5] and assign to $\Delta H°_7$ the typical value of –130 kJ/mol (–31 kcal/mol) for unconstrained $OH^+ \cdots O$ dimers. Substituting these values in eq 1 gives $\Delta H°_8$, i.e., the interaction energies of the free ether groups with the charged centers. In $(G1)_2H^+$ (ion III above) this extra stabilization energy is only –17 kJ/mol (–4 kcal/mol). Again, the strained geometry apparently prevents efficient alignment of the dipoles of the unbound ether groups. On the other hand, in $(G2)_2H^+$ (ion IV above), eq 1 gives $\Delta H°_8$ as –54 kJ/mol (–13 kcal/mol). The increased stabilization in this case can be attributed to the greater freedom of the terminal ether groups in approaching the charged center, as well as the larger number of free ether groups in this particular complex.

An alternative to ion IV may be a structure such as IV′ in which the strong intramolecular ionic H-bond in $G2H^+$ remains intact and the second G2 molecule complexes the proton by two weak 'T-shaped' hydrogen bonds in an out-of-plane (perpendicular) configuration. By analogy with $(CH_3)_2OH^+ \cdots CH_3OH$, each of these bonds could contribute 42 kJ/mol (10 kcal/mol).[2,3] The measured thermochemistry may be compatible with either ion IV or IV′, although IV is probably favored at higher temperatures due to entropy factors.

Complexing of H_3O^+ by Polyethers. First, we note that in these complexes the proton may be associated with the H_3O^+ moiety, although the ether groups have higher proton affinities by more than 146 kJ/mol (35 kcal/mol).[24] The proton may be incorporated as H_3O^+ because of the opposing attractions of the ligand groups, analogous to the complexes of H_3O^+ with several MeCN,[25] Me_2CO,[26] and Me_3N[27] molecules, and of NH_4^+ with Me_3N molecules.[28]

Experimentally we monitor the equilibria associated with the addition of H_2O to protonated polyethers, reaction 5. The thermochemistry as shown in Table 1 is similar to that of the analogous reaction of monofunctional ions such as Me_2COH^+ and $n\text{-}Pr_2OH^+$, due to the canceling effects of dissociating the

(24) Izatt, R. M.; Haymore, B. L.; Christensen, J. J. *J. Chem. Soc., Chem. Commun.* **1972**, 1308.
(25) Deakyne, C. A.; Meot-Ner (Mautner), M.; Campbell, C. L.; Hughes, M. G.; Murphy, S. P. *J. Chem. Phys.* **1986**, *84*, 4958.
(26) Tzeng, W. B.; Wei, S.; Neyer, D. W.; Keesee, R. G.; Castleman, A. W. *J. Am. Chem. Soc.* **1990**, *112*, 4097.
(27) Wei, S.; Shi, Z.; Castleman, A. W. *J. Chem. Phys.* **1991**, *94*, 3268.
(28) Wei, S.; Tzeng, W. B.; Castleman, A. W. *J. Chem. Phys.* **1991**, *95*, 585.

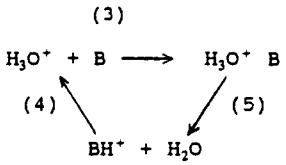

internal hydrogen bonds in the protonated polyethers and of forming multiple bonds in the complexes (see discussion below).

The thermochemistry for the complexing of H_3O^+ by the polyethers, reaction 3, was obtained from the experimental data in Table 1 using a thermochemical cycle and protonation thermochemistry.[21] Results are summarized in Table 2.

With the exception of $G1H^+ \cdot H_2O$, which is bonded more weakly than the other complexes, (see below) the other complexing energies for H_3O^+ are divided primarily into two groups. The first includes G2 and G3, which complex H_3O^+ by 310–352 kJ/mol (74–84 kcal/mol), similar to the addition of two Me_2CO molecules. It may be assumed that all of these are bidentate complexes, as in structures **V** and **VI**.

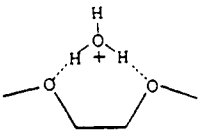

V

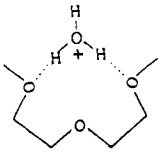

VI

The $\Delta S°$ values are more negative than the typical −105 to −126 J/(mol K) (−25 to −30 cal/(mol K)) associated with the formation of unconstrained $BH^+ \cdots B$ complexes, which also suggests cyclic structures consistent with **V** and **VI**. However, they are not as negative as those found for tridentate complexes. The two optimized hydrogen bonds with H_3O^+ evidently pucker the G2 molecule in a manner that prevents the free ether group from forming a third hydrogen bond. When G3 bonds H_3O^+, the linkage apparently involves the two terminal ether groups, forming a larger ring, and the geometries may optimize. This premise is supported by the similarity of the complexing energy to that in $H_3O^+ \cdot 2G1$, where the two separate G1 molecules can also be oriented to optimize the hydrogen bond alignment. The complex with 15-crown-5 also shows somewhat enhanced bonding, and Sharma and Kebarle suggested a partial third hydrogen bond in this case.[3]

The second group in Table 2 shows significantly stronger complexing and significantly more negative $\Delta S°$ values, with a thermochemistry similar to that associated with the three hydrogen bonds in $H_3O^+ \cdot 3Me_2CO$. These may be considered as tridentate complexes, as in **VII** and **VIII**.

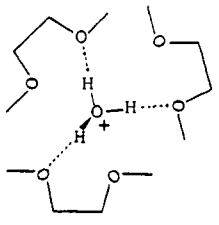

VII

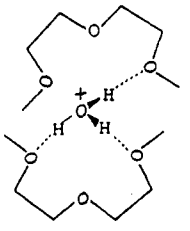

VIII

Comparison of tridentate complexes containing six ether groups confirms that three G1 or two G2 molecules bind H_3O^+ more strongly than an 18-crown-6 molecule. As in the complexing of the proton, this suggests that the hydrogen bonds are more optimized when there are several free ether molecules in the complex. The polyether complexes are also further stabilized by the dipoles of the nonbonded ether groups.[3] For example, the bonding is tighter than that found for three H-bonds to three Me_2CO molecules. However, these interactions are apparently not fully optimized, as indicated by the fact that the bonding is substantially less than that estimated for incorporating six carbonyl functions as Me_2CO ligands (Table 2).

Energy Factors in the H_3O^+ Complexes. The thermochemistry can also be used to assign specific energy contributions in the complexing of H_3O^+ within ions such as **V** and **VI**. A hypothetical three-step process for complex formation can be written as reactions 10–12.

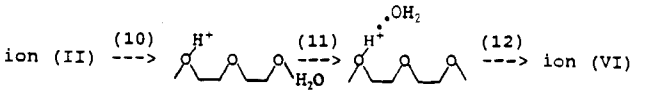

For reaction 10 we again assign the internal IHB thermochemistry from previous work,[5] and for reaction 11, which forms a simple monodentate $OH^+ \cdots OH_2$ complex, we use the appropriate $\Delta H°$ from proton affinity correlations for such complexes.[29] Assigning a proton affinity of 837 kJ/mol (200 kcal/mol) to the ether groups gives $\Delta H°_{11} = -92$ kJ/mol (−22 kcal/mol), and from analogous clustering reactions, such as those for $Me_2COH^+ + H_2O$ and $n\text{-}Pr_2OH^+ + H_2O$ (Table 1), we can estimate $\Delta S°_{11} = -105$ J/(mol K) (−25 cal/(mol K)). These considerations give for the second bond in the $G1 \cdot H_3O^+$ (ion **V**), $G2 \cdot H_3O^+$ (ion **VI**), and $G3 \cdot H_3O^+$ complexes $\Delta H°_{12} = -25$ (−6), −92 (−22), and −113 (−27) kJ/mol (kcal/mol) and $\Delta S°_{12} = -17$ (−4), −100 (−24), and −142 (−34) J/(mol K) (cal/(mol K)), respectively. The thermochemistry therefore shows inefficient interaction of the second ether group with H_3O^+ in the $G1 \cdot H_3O^+$ complex, and our ab initio calculations indicate that the singly and doubly bonded conformations are of comparable energy.

In $G2 \cdot H_3O^+$ and $G3 \cdot H_3O^+$ the complexing energy associated with the second ether group is comparable to the attachment energy of a second free ligand molecule in $(H_3O^+ \cdot Me_2CO) + Me_2CO$, which is 88 kJ/mol (21 kcal/mol),[10] suggesting that the large ring structures allow a fully optimized geometry for the second bond, with added stabilization provided by the additional dipoles in G3·H3O+. The fact that the second ether group bonds as strongly as a free ligand also indicates that the protonation or hydrogen-bonding interactions of the first ether group do not significantly affect the charge density on the second ether group.

As found for complexing of the proton, entropy changes can oppose the enthalpy differences in the various complexes. For example, in the combinations with six polar groups in Table 2, three G1 and two G2 molecules bind H_3O^+ more strongly than 18-crown-6. However, the crown ether complex is the most stable in terms of $\Delta G°_{300}$ due to entropy effects.

Mixed Clusters of G1 and H_2O. The thermochemical network derived for $(G1)_n(H_2O)_mH^+$ complexes is given in Figure 6. The most interesting complex is $G1 \cdot (H_2O)H^+$, which may exhibit a solvent-bridged structure. Figure 7 indicates that the enthalpy sequence for adding H_2O molecules to $G1H^+$ shows an anomalous contour compared with the sequences for several monofunctional ions. The first attachment energy is lower by about 17 kJ/mol (4 kcal/mol) than may be expected from $\Delta PA/\Delta H°_D$ correlations,[29] due to the internal stabilization of the monomer $G1H^+$ ion as noted in reactions 10–12. However, the second solvation step is stronger by approximately 11 kJ/mol (2.5 kcal/mol) than in hydration sequences of monofunctional ions such as $Me_2COH^+ \cdot 2H_2O$, $(HCONH_2O)H^+$, etc,[29] suggesting that a bridged structure is formed between the two ether groups, as in ion **XI**. The thermochemistry of this reaction was investigated in four separate measurements with H_2O concentrations varying between 0.085 and 0.89%, and the results (see Figure 1) yield $\Delta H° = -65.2 \pm 1.3$ kJ/mol (−15.6 ± 0.3 kcal/mol) and $\Delta S° = -117.0 \pm 2.1$ J/(mol K) (−28.0 ± 0.5 cal/(mol K)), with standard deviations as indicated. Given the precision, the discontinuity

(29) Meot-Ner (Mautner), M. *J. Am. Chem. Soc.* **1984**, *106*, 1265.

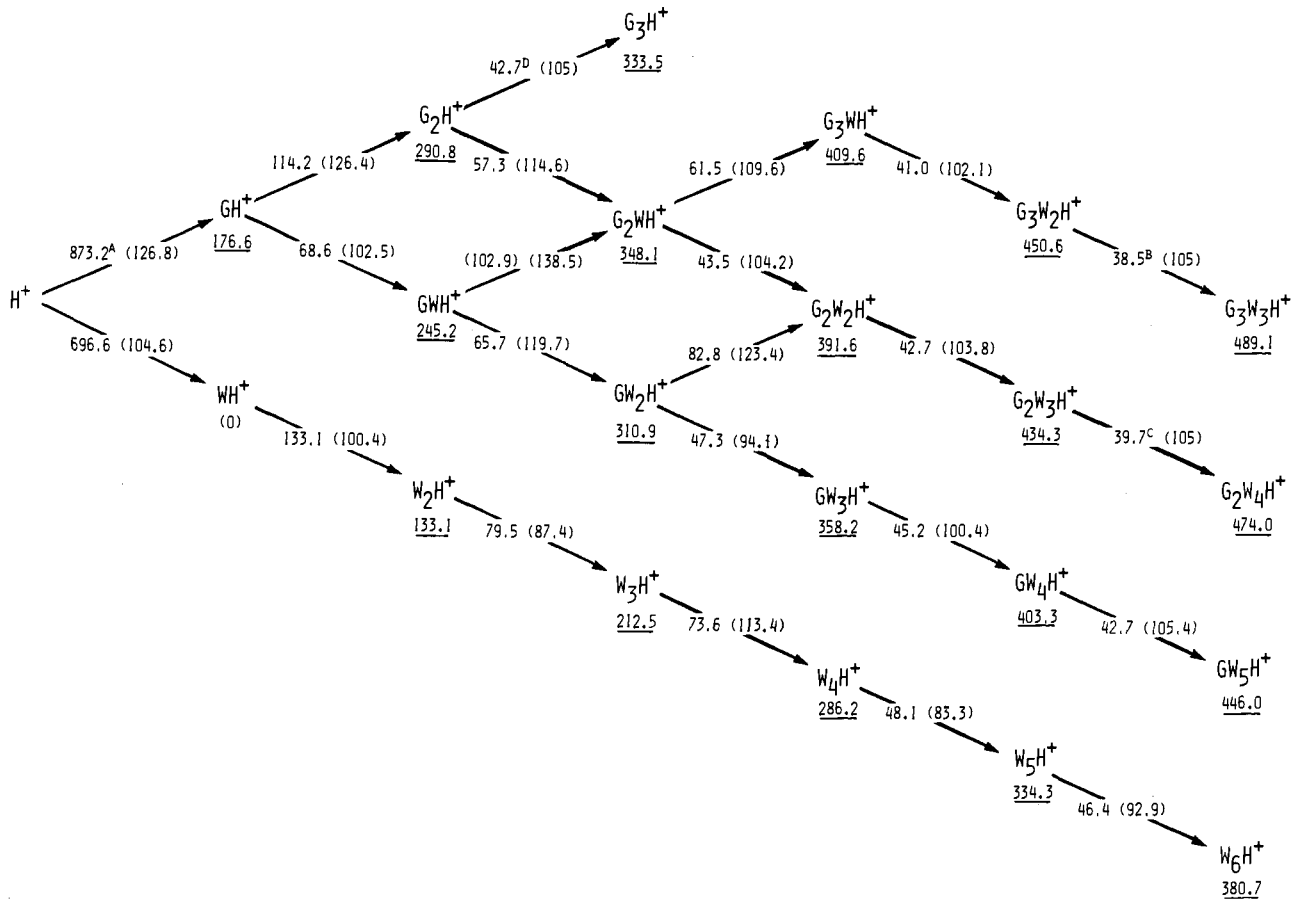

Figure 6. $\Delta H°$ in kJ/mol and, in parentheses, $-\Delta S°$ in J/(mol K) for clustering and switching reactions in glyme/water mixtures. Underlined values below the ions indicate the total dissociation enthalpy for $G_nW_mH^+ \leftrightarrow WH^+ + nG + (m-1)W$. Nomenclature is the same as in Figures 1 and 2. Superscripts are as follows: (A) adjusted to the new proton affinity scale (ref 13); (B) from $\Delta G°_{225} = -14.6$ kJ/mol; (C) from $\Delta G°_{225} = -16.3$ kJ/mol; (D) from $\Delta G°_{208} = -20.9$ kJ/mol.

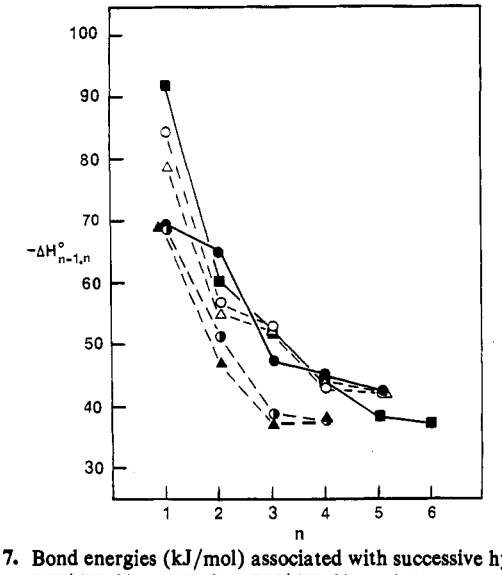

Figure 7. Bond energies (kJ/mol) associated with successive hydration of the type $BH^+(H_2O)_{n-1} + H_2O \leftrightarrow BH^+(H_2O)_m$ as follows: ●, glymeH$^+$ (1,2-dimethoxyethaneH$^+$); ○, $(CH_3)_2COH^+$; △, $(n\text{-}C_3H_7)_2OH^+$; ◐, $CH_3(N(CH_3)_2)COH^+$; ▲, $(c\text{-}C_3H_5)_2COH^+$. Values denoted by ■ are for glymeH$^+$(MeOH)$_{n-1}$ + MeOH ↔ glymeH$^+$(MeOH)$_n$.

between G1 and the monofunctional bases at $n = 2$ appears to be meaningful. The second H_2O molecule then fills the first shell, and the next attachment energies are typical of outer shell attachment energies. Increased bond strength is absent in the $(G1)(MeOH)_nH^+$ series at $n = 2$, where delocalization of the charge to the methyl groups may destabilize the bridged structure.

In mixed complexes of the type $(G1)_m(H_2O)_nH^+$, we find increasing stabilization with increasing G1 content for clusters of a given rank r (where $r = m + n$), up to compositions $m = n + 2$, after which further hydrogen bonds are blocked. This trend is similar to that found for $(Me_2O)_m(H_2O)nH^+$, $(Me_2CO)_m(H_2O)H^+$, and $(MeCN)_m(H_2O_nH^+)$ complexes. We also note the effect of blocking in the weak bond associated with the third G1 molecule to form $(G1)_3H^+$. One might expect that the intermolecular bonds in higher complexes displace the weak internal bond in G1H$^+$ or the weak cyclic structures in $(G1)(H_2O)H^+$ or $(G1)(H_2O)_2H^+$. However, the thermochemical trends in the higher clusters are quite similar to those found for $(Me_2O)_m(H_2O)_nH^+$, $(Me_2CO)_m(H_2O)_nH^+$, and $(MeCN)_m(H_2O)_nH^+$ aggregates.

Clusters of G2H$^+$ and G3H$^+$ with Several H_2O Molecules. The thermochemistry for addition of a second H_2O molecule to the bidentate complex G2·H$_3$O$^+$, $\Delta H° = -54.8$ kJ/mol (−13.1 kcal/mol) and $\Delta S° = -97.1$ J/(mol K) (−23.2 cal/(mol K)), is very similar to that determined for addition of H_2O to the evidently bidentate complex H_3O^+·2Me$_2$CO, where $\Delta H° = -58.2$ kJ/mol (−13.9 kcal/mol) and $\Delta S° = -114.2$ J/(mol K) (−27.3 cal/(mol K)),[10] which is consistent with the conclusion that H_3O^+·G2 is a bidentate complex. The second H_2O molecule then completes the inner shell about the H_3O^+ core ion as in ion **IX**, and the third H_2O molecule simply ads to begin an outer shell. Indeed, the small attachment energy of the third H_2O molecule ($-\Delta H° < 42$ kJ/mol (10 kcal/mol)) is similar to the typical attachment energies of outer shell H_2O molecules in hydrated clusters,[30] such as in the Me_2COH^+·nH$_2$O and n-Pr_2OH^+·nH$_2$O series (Table 1).

(30) Keesee, R. G.; Castleman, A. W. *J. Phys. Chem. Ref. Data* **1986**, *15*, 1011.
(31) Yamabe, S.; Hirao, K.; Wasada, H. *J. Phys. Chem.* **1992**, *96*, 10261.

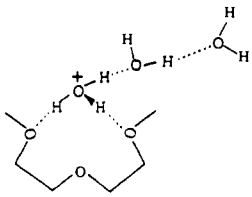

IX

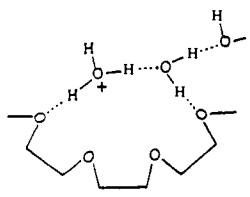

X

A substantial entropy change is observed in the $G3H^+ \cdot H_2O + H_2O$ system. The $\Delta S°$ value of −132.6 J/(mol K) (−31.7 cal/(mol K)) is large compared with typical values of −100 ± 8 J/(mol K) (−24 ± 2 cal/(mol K)) for adding consecutive H_2O molecules to monodentate ions,[30] such as in the $n\text{-}Pr_2OH^+ \cdot nH_2O$ series (Table 1). The second H_2O molecule may be constrained in a multiply complexed structure, as in ion **X**, which completes the inner shell. Accordingly, the attachment energies of −43.1 and −38.1 kJ/mol (−10.3 and −9.1 kcal/mol) for the third and fourth H_2O molecules are typical outer shell attachment energies.[29,30]

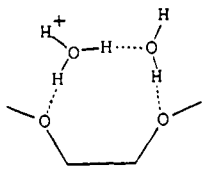

XI

The bridged structures **X** and **XI** are of interest as models of proton wires in biological membranes, such as the one proposed to account for high proton mobility in the gramicidin channel.[33,34] The present observations suggest that these bridged structures may indeed be stable. The biological implications of these cluster models will be discussed in detail elsewhere.[10]

Ab Initio Calculations. A. Protonation. Calculations were also performed on the dihydroxyethane (DHE) molecule illustrated in Figure 8, which was chosen as a model system due to computational ease as well as eliminating initial complications of methyl rotations. The neutral (**8a**) contains an internal H-bond, albeit a weak one, due to the rigidity of the molecular skeleton. Protonation of DHE leads to structure **8b**, which contains a significantly strengthened H-bond. The $r(H\cdots O_2)$ distance contracts from 2.36 to 1.74 Å upon protonation. Part of the closer approach of these two atoms arises from a reduced $\phi(O_1CCO_2)$ dihedral angle in the protonated species. The electronic contribution to the binding energy of DHE with the proton is calculated to be 881.6 kJ/mol (210.7 kcal/mol), as listed in the first entry in Table 3. Addition of zero-point vibrational energy reduces this quantity to −853.3 kJ/mol (202.5 kcal/mol). The experimental proton affinity has not been determined due to the fact that $DHEH^+$ readily dehydrates, even at moderate temperatures, but our best estimate for $\Delta H°$ at 298 K is −853.1 kJ/mol (−203.9 kcal/mol). The other thermodynamic quantities of interest are also listed in Table 3. Calculations indicate that the protonation of O_1 increases its electron density as well as that of the other oxygen. The negative charge on O_1 is increased from −0.757 to −0.806. The internal H-bond is quite clearly asymmetric with $r(OH)$ distances of 0.983 and 1.736 Å.

Similar computations were also performed for G1, in which the terminal H atoms on each oxygen of DHE are replaced by methyl groups. As is clear from comparison of Figures 8a and 9a, the equilibrium structure of G1 differs from that of DHE in that the two methyl groups are both turned out away from the middle of the molecule. The absence of the H-bond in G1 allows the $\phi(O_1CCO_2)$ dihedral angle to increase. The electronic part

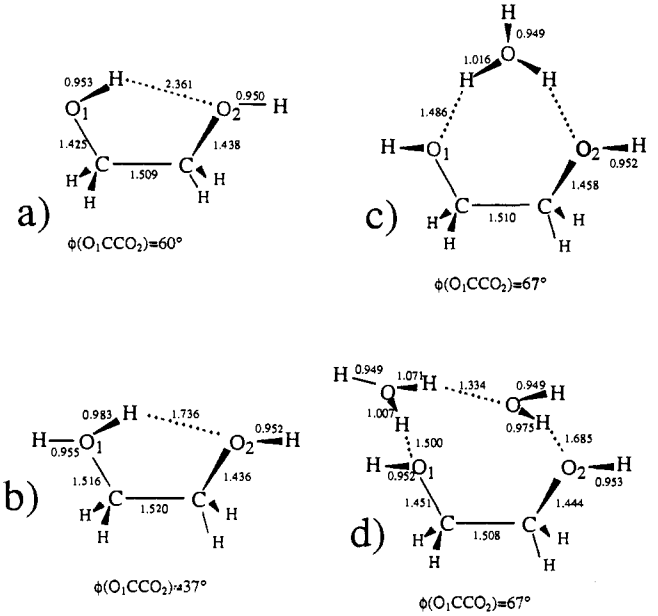

Figure 8. Computed optimal geometries in DHE, $DHEH^+$, and proton-bound hydrates. See text for details.

Table 3. Computed Thermodynamics of Association Reactions

	DHE + H^+		$DHEH^+ + H_2O$		$DHEH^+ \cdot H_2O + H_2O$	
	kJ/mol	kcal/mol	kJ/mol	kcal/mol	kJ/mol	kcal/mol
E_{elec}	−881.6	−210.7	−136.4	−32.6	−101.3	−24.2
E_{elec} + ZPVE	−847.3	−202.5	−127.2	−30.4	−88.7	−21.2
$\Delta H°$	−853.1	−203.9	−131.4	−31.4	−93.3	−22.3
$\Delta S°$ [b]	−107.5	−25.7	−135.6	−32.4	−142.7	−34.1
$\Delta G°$	−821.3	−196.3	−90.8	−21.7	−50.6	−12.1
	G1 + H^+		$G1H^+ + H_2O$		$G1H^+ \cdot H_2O + H_2O$	
	kJ/mol	kcal/mol	kJ/mol	kcal/mol	kJ/mol	kcal/mol
E_{elec}	−944.3	−225.7	−102.9	−24.6	−95.8	−22.9
E_{elec} + ZPVE	−907.5	−216.9	−97.1	−23.2	−82.0	−19.6
$\Delta H°$	−913.4	−218.3	−101.7	−24.3	−86.2	−20.6
$\Delta S°$	107.5	−25.7	−136.0	−32.5	−146.9	−35.1
$\Delta G°$	−881.2	−210.6	−61.1	−14.6	−42.3	−10.1

[a] All at 298 K. [b] Units J/(mol K) and cal/(mol K).

of the proton affinity of G1 is 944.3 kJ/mol (225.7 kcal/mol), some 7% less than that calculated for DHE. Following vibrational and other corrections, $\Delta H°$ is calculated to be 881.2 kJ/mol (210.6 kcal/mol), only a little larger than the experimental measurement of 854 kJ/mol (204 kcal/mol).[5]

Yamabe et al.[31] have recently reported ab initio calculations for a number of initernally H-bonded species, including $G1H^+$. The geometry they optimized with the 3-21G basis set describes a somewhat more compact molecule with a shorter H-bond than obtained here using 4-31G. These differences are consistent with the large basis set superposition error characteristic of 3-21G, which would tend to impose an artificially enhanced attraction within the molecule.[32]

The internal H-bond in $G1H^+$ appears comparable to that in $DHEH^+$ from a geometric standpoint; $r(H\cdots O_2)$ is within 0.02 Å in the two ions (cf. Figures 8b and 9b).

B. Hydration Energetics. Addition of a single water molecule to $DHEH^+$ leads to the symmetric structure in Figure 8c. Note that the proton transfers to the water immediately upon its addition, probably because the H_3O^+ species can form H-bonds to both O atoms of DHEH. The stretching of the internal $r(OH)$ bond lengths to 1.016 Å, coupled with the short intermolecular $r(H\cdots O)$ distances of only 1.486 Å, indicates quite a strong

(32) Sordo, J. A.; Sordo, T. L.; Fernandez, G. M.; Gomperts, R.; Chin, S.; Clementi, E. *J. Chem. Phys.* **1989**, *90*, 6361.
(33) Deamer, D. W. *J. Bioenerg. Biomembr.* **1987**, *19*, 457.
(34) Deamer, D. W.; Nichols, J. W. *J. Membr. Biol.* **1989**, *107*, 91.

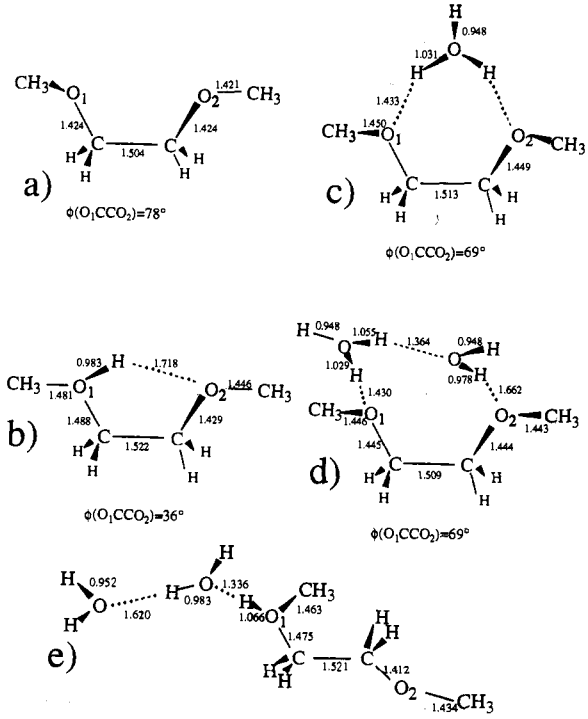

Figure 9. Computed optimal geometries in G1H$^+$ and proton-bound hydrates. See text for details.

interaction. Indeed, this complex is stabilized by 136.4 kJ/mol (32.6 kcal/mol), relative to the protonated DHE plus a neutral water. Consideration of zero-point vibrational energies reduces the binding energy to 127.2 kJ/mol (30.4 kcal/mol).

The interaction between G1H$^+$ and water is found to be slightly weaker than that computed for DHEH$^+$. Comparison of Figures 8c and 9c reveals that the r(H··O) distance shrinks to 1.433 Å, whereas the energetics in Table 3 indicate an approximately 33.5 kJ/mol (8 kcal/mol) reduction in the interaction energy. The calculated value of $-\Delta H°$ is 100 kJ/mol (24 kcal/mol) for binding of the water molecule, somewhat larger than the experimental estimate of 68.6 kJ/mol (16.4 kcal/mol).

The most stable structure corresponding to the addition of a second water to DHEH$^+$ is depicted in Figure 8d. It is worth stressing that the excess proton remains on the first water and there is now a network of H-bonds present. Using the interatomic distances as a criterion, the bond between H_3O^+ and O_1 is slightly weaker here, since r(OH) has contracted to 1.007 Å and r(H··O) is slightly longer at 1.50 Å. The weakest bond of the three connects the neutral water to O_2. Altogether, the binding energy of this complex, relative to DHE··H_3O^+ in Figure 8c plus another neutral water, is 101.3 kJ/mol (24.2 kcal/mol), reduced to 88.7 kJ/mol (21.2 kcal/mol) by vibrational energy.

Addition of a second water molecule to the G1H$^+$···H_2O complex yields much the same complex as for the DHE system. The H_3O^+ species approaches O_1 more closely, and the other water is closer to O_2 whereas the two water oxygens move further apart in the complex with G1. Table 3 indicates the binding energy of the second water is about 8 kJ/mol (2 kcal/mol) less than in the case of DHE. The calculated value of $-\Delta H°$, 86.2 kJ/mol (20.6 kcal/mol), is again somewhat larger than the experimental measurement of 65.7 kJ/mol (15.7 kcal/mol).

One last point that was tested was the comparative stability of the "closed" dihydrated complex in Figure 9d, as compared to an open form. The geometry of such an open form is illustrated in Figure 9e and is interesting first from the perspective that the excess proton now remains on the G1 rather than on either water molecule. On the other hand, this structure is less stable than the closed form by 33.5 kJ/mol (8.0 kcal/mol). Inclusion of vibrational contributions has little effect on this competition, leaving the energy difference virtually unchanged. One might expect the open form might be favored at higher temperature due to its supposed higher entropy. In fact, the difference in entropy between the two geometries is only 49.4 J/(mol K) (11.8 cal/(mol K)). When combined with a difference in enthalpy of 35.1 kJ/mol of (8.4 kcal/mol) at 298 K, one obtains a free energy difference of 20.5 kJ/mol (4.9 kcal/mol) favoring the closed form.

The most significant feature of the calculations is not necessarily the agreement with experiment in terms of absolute numbers but rather the fact that the computed enthalpies for addition of the first and second H_2O molecules to G1H$^+$ differ by a relatively small amount, 17 kJ/mol (4 cal/mol). Considering the combined evidence, it is apparent that the excess proton is located on the cluster component having the lower proton affinity (the first water molecule), which is then H-bonded to both G1 and the second water; i.e., G1H$^+$ ceases to be the core ion. Models such as these provide facile building blocks for the development of proton wires in complex hydrated systems, which could result from charge migration, via proton shifts, away from highly basic functions and incorporation into more stable H-bonded bridges involving $H^+(H2O)_n$.

Conclusions

The present results extend the data on polydentate ionic hydrogen bonding. The complexing of H$^+$ involves the formation of intramolecular or intermolecular hydrogen bonds, whose strengths increase as the geometry of the OH$^+$··O bond can be better optimized. The bonding of H_3O^+ can involve two or three hydrogen bonds. Both the complexes of H$^+$ and H_3O^+ are further stabilized by interactions with bond dipoles of free ether groups of the polyether molecules, and this stabilization increases with decreasing constraints on the geometries of the polar groups. Such interactions are not significant in the complexes of the constrained G1 molecule, but in the complexes of larger ethers they contribute up to 54 kJ/mol (13 kcal/mol).

The protonated systems contain several polar groups and a limited number of solvent molecules, simulating the environment in protein interiors. The present experiments and calculations verify that the protonated water bridge is stable in G1H$^+$·2HO. This suggests that similar bridges proposed in the gramicidin channel may also be stable.[11,24,33] Also relevant is the fact that the proton remains on the water molecules, as the calculations show. A similar structure may explain that the proton can move through the gramicidin chain without being trapped by the peptide carbonyls, which have higher group proton affinities.

Acknowledgment. This work was funded in part (L.W.S.) by the Office of Chemical Sciences, Division of Basic Energy Sciences, US Department of Energy. The group at SIU was supported by the National Institutes of Health (Grant GM29391). We are also deeply indebted to one of the reviewers of the original version of the manuscript, who carried out RHF/4-31G computations on G1·2H_2O and found the bridged form to be the most stable. The reviewer's effort prompted us to perform a full geometry optimization, which resulted in minima on the potential surface and permitted calculation of the associated thermodynamic quantities. We are also deeply indebted to Ms. Pamela Christian of NIST for her help in preparing the manuscript.

Appendix—Confirmation of Equilibrium

The formation of protonated dimers in polyethers and the association equilibria were investigated at reduced temperatures in order to minimize pyrolysis reactions. As a result, low reactant concentrations were sometimes required, and it is important to demonstrate that true equilibrium was achieved under these rather adverse (dilute) conditions. For this purpose, we will present and describe some experimental ion profiles and discuss the consistency

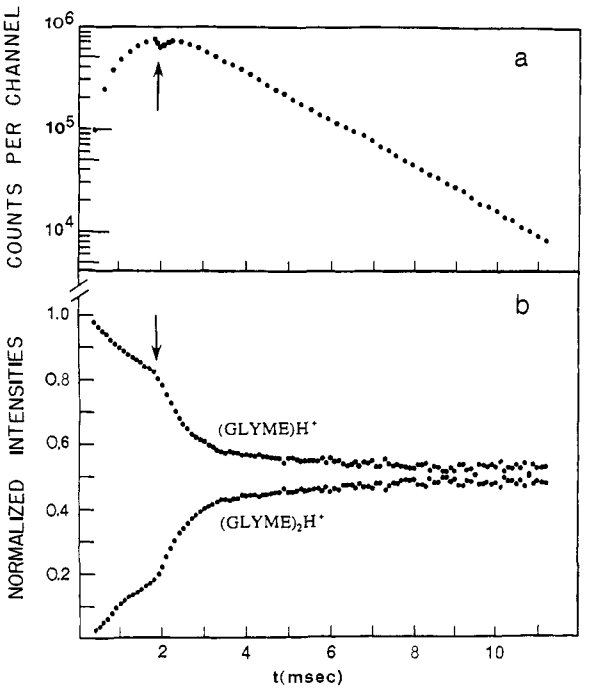

Figure 10. Total ion intensities (a) and normalized data (b) found for the pulsed ionization of a CH_4/G1 mixture. See Appendix for details.

of the dimerization thermochemistry measured at various concentrations.

Figure 10 displays experimental data obtained from the pulsed ionization of a mixture containing 2.3×10^{-5} mole fraction (m.f.) glyme in methane at 435 K (total pressure 3.7 mbar). Part a gives the total ion current observed for $G1H^+$ and $(G1)_2H^+$ as a function of time from initiation of the electron pulse to approximately 11 ms. No other ions comprising more than 1% of the total ionization were detected at long reaction times. Intensities were accumulated in 20-μs-wide channels, and the ionizing pulse was terminated at approximately 1.9 ms. Data is shown for every tenth channel. Part b of Figure 10 gives the temporal normalized intensities (fraction of total ionization) for $G1H^+$ and $(G1)_2H^+$ over the same analysis time (data shown for every fifth channel). The slow, but steady, approach to equilibrium following termination of the electron pulse is clearly indicated in the range 2–7 ms, and the equilibrium ion intensities were taken as those recorded from 7.5 to 11.2 ms in this particular measurement, which was taken at extremely low concentration in order to minimize further clustering. The observed ion ratio corresponds to a ln K of 16.21 for the dimerization reaction. It is apparent that true equilibrium is obtained at long reaction times even under these very unfavorable conditions. At higher temperatures, equilibrium was usually obtained at much shorter analysis times in mixtures of similar concentration.

Figure 11 gives the time-resolved normalized intensities for $G2H^+$ and $(G2)_2H^+$ found in a mixture containing 4.1×10^{-5} m.f. G2 in CH_4 at 321 K and at a total pressure of 3.7 mbar (20-μs-channels, every tenth channel displayed). Again, the

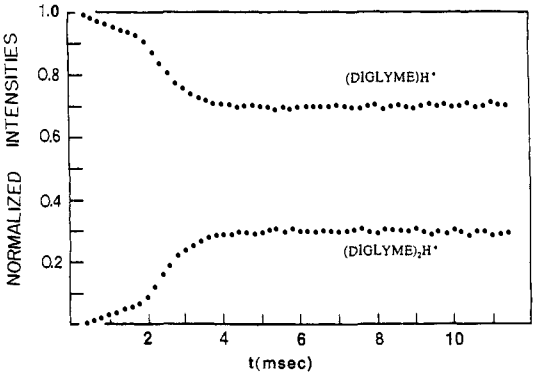

Figure 11. Normalized data for pulsed ionization of a CH_4/G2 mixture. See Appendix for details.

approach to equilibrium is apparent after termination of the electron pulse at 1.8 ms. Because a slightly higher concentration of reactant was used in these particular measurements, equilibrium was reached at a total analysis time of approximately 5–6 ms (compare with Figure 10b). The equilibrium ion ratio corresponds to a K_{equil} of 14.85 at this temperature. These data are presented to verify that the association equilibria discussed in this study can be reliably evaluated in spite of unfavorable temperature and concentration requirements. The vast majority of our measurements are typically conducted under much more benign conditions.

To confirm that the derived thermochemistry was independent of reactant concentration for those systems which presented the most stringent experimental requirements, we carried out detailed temperature studies in mixtures with various concentrations at constant total pressures in the range 2.5–5.0 mbar. For the $(G1)_2H^+$ measurements, data were taken at the following m.f.'s of G1 and temperature ranges (K) (1.5×10^{-5} (440–484); 2.3×10^{-5} (419–467); and 4.5×10^{-4} (467–515)), giving the following $\Delta H°$ (kJ/mol (kcal/mol)) and $\Delta S°$ (J/mol K) (cal/(mol K))) values, respectively (116.7 (27.9), 125.5 (30.0); 115.5 (27.6), 131.0 (31.3); and 115.5 (27.6), 133.8 (32.0)). For $(G2)_2H^+$, measurements were at m.f.'s and temperature ranges as follows (4.3×10^{-5} (328–379); 2.5×10^{-4} (327–357); and 4.1×10^{-4} (309–361)), giving the following thermochemistry ($\Delta H°$ and $\Delta S°$) (92.0 (22.0), 157.8 (37.7); 84.9 (20.3), 151.9 (36.3); and 90.4 (21.6), 166.9 (39.9). Concentrations in both systems were varied over 1 order of magnitude, and the respective results were consistent within the usual reproducibility associated with HPMS clustering measurements and show no systematic changes with concentration. Average values reflecting all of the results are given in Table 1 for each individual ether.

Pyrolysis of n-Pr_2OH^+ generates the i-Pr^+ ion in the $(n\text{-}Pr_2O)_2H^+$ system, which further reacts with n-Pr_2O via proton transfer to initiate steady-state cycles. This situation occurs in the temperature range (420–550 K) where the protonated monomer/dimer ratio reaches constant values during the analysis time. As a result of this complication, the apparent equilibrium constant was pressure dependent. Evaluation of the thermochemistry in this particular case resulted from low-temperature studies (320–400 K) using ligand-switching reactions involving $(Et_2CO)_2H^+$ (see Table 1 for details).